

## P1.11 A COMPARISON OF HIGH-RESOLUTION ICE-OCEAN MODEL RESULTS WITH SHEBA DATA

Wieslaw Maslowski<sup>1</sup>, Anastasia Romanou<sup>2</sup>, David M. Holland<sup>2</sup>, Jaclyn L. Clement<sup>1</sup>, Waldemar Walczowski<sup>3</sup>  
<sup>1</sup>Naval Postgraduate School, Monterey, CA 93943, <sup>2</sup>Courant Institute of Mathematical Sciences, New York University, New York, NY 10012, <sup>3</sup>Institute of Oceanology, Polish Academy of Sciences, Sopot, Poland

### 1. INTRODUCTION

The SHEBA (Surface Heat Budget of the Arctic Ocean) project took place in the western Arctic Ocean from October 1997 to October 1998. Its mission was to collect concurrent data for several atmospheric, sea ice and oceanic fields over an annual cycle. This field experiment provided an extensive ensemble of concurrent data sets that describe mass, energy, heat and turbulent flux exchanges between the atmosphere, ice and ocean interfaces (Uttal et al., 2002).

In this study we use some of the SHEBA observations to compare with results from a high resolution coupled ice-ocean model of the Pan-Arctic region (Maslowski and Walczowski, 2002) forced with realistic atmospheric fields from the European Centre for Medium-range Weather Forecast (ECMWF).

First we compare the SHEBA data for the atmosphere with the ECMWF operational products prescribed to the model for the same period. The model forcing fields include the radiative fluxes, 2-m air temperature and dew point. In addition, the air-ocean horizontal stresses at the surface were calculated from the 10-m wind fields. All the atmospheric parameters are interpolated from the original ECMWF locations to the model  $1/12^\circ$  ( $\sim 9$  km) rotated spherical grid.

Next we will compare the ice and ocean fields that are produced from a model that is run using ECMWF forcing with the SHEBA measurements. Both the annual cycle and selected time intervals over the SHEBA period are derived from the model for validation with data. Model-data discrepancies are quantified and their possible sources are hypothesized. In addition, model results are analyzed in attempt to synthesize the SHEBA experiment into a 'larger picture' of oceanic circulation and variability.

### 2. THE NPS MODEL

A new high-resolution ice-ocean model of the Pan-Arctic region has been developed and tested at the Naval Postgraduate School. The initial emphasis of this work was on improvements in sea ice leading to better prediction of open water regions, i.e. leads and polynyas within the ice pack. Ability to predict such narrow (of order  $O(10\text{km})$ ) and long (of order  $O(1000\text{km})$ ) features in the sea ice is of interest and importance to operational oceanography and climate change studies.

One of the requirements to advance ice model predictive skill involved increasing model horizontal grid cell resolution. The model grid was configured at  $\sim 9$  km and 45 levels using the rotated coordinate system to eliminate singularity problem at the North Pole.

The model domain extends from the North Pacific ( $\sim 30^\circ\text{N}$ ), over the Arctic Ocean, the Canadian

Archipelago and the Nordic Seas, to the North Atlantic (to  $\sim 45^\circ\text{N}$ ). This approach allows accounting for all the northern latitude ice covered regions at a high and nearly uniform resolution. This research is an extension of our previous modeling work (Maslowski et al., 2000, Maslowski et al., 2001).

Model improvements have been so far tested in two steps. The first test was designed to examine the effects of higher resolution on the existing ice model coupled to an ocean model with more realistic bathymetry. A 70-year integration of the coupled ice-ocean model has been completed. This model run has been forced with daily-averaged realistic atmospheric fields from the European Centre for Medium-range Weather Forecasts (ECMWF) 1979-1993 reanalysis and operational products for 1994-2001. The coupled model adapts the Los Alamos National Laboratory (LANL) Parallel Ocean Program (POP) ocean model with a free surface. The sea ice model uses a viscous-plastic rheology, the zero-layer approximation of heat conduction through ice and a simplified surface energy budget. Many improvements, such as the ice edge position in the Nordic and Bering/Chukchi Seas, are results of more realistic modeling of the upper ocean currents and hydrography. Some results from this experiment are at [www.oc.nps.navy.mil/~pips3](http://www.oc.nps.navy.mil/~pips3).

The second test has focused on evaluating the new sea ice model ability to predict leads and polynyas. A 20-year integration of the stand-alone 9-km sea ice model with a mixed ocean layer has been completed. This model uses the most recent version of sea ice model (CICE 3.0) developed at LANL. It contains an improved calculation of ice growth/decay based on work of Bitz and Lipscomb (1999). It has been configured to

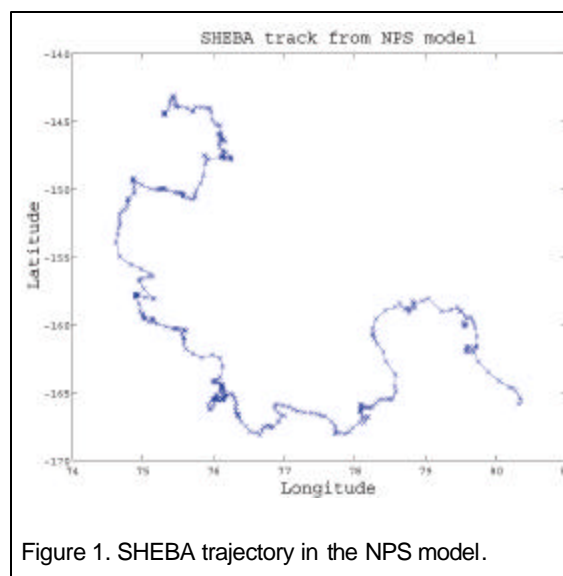


Figure 1. SHEBA trajectory in the NPS model.

use five sea ice categories with 4 layers per category, a snow layer in each category, the EVP rheology (Hunke and Dukowicz, 1997), the remapping of sea ice transport (Lipscomb and Hunke, 2002) and ice thickness (Lipscomb, 2001). The realistic daily-averaged 1979-1988 ECMWF atmospheric data has been used to force the model. Results on model representation of leads and polynyas over the Chukchi/Beaufort Sea region will be presented, including sea ice concentration, drift, divergence, shear, and vorticity. Further model evaluations are planned as results from integration of the new sea ice model coupled to the pan-Arctic ocean model become available.

### 3. DATA ANALYSIS

#### 3.1 Atmospheric Data

SHEBA data from the Atmospheric Surface Flux Group (ASFG) tower is used for the comparison (Persson et al., 2001). Near-surface environment including wind speed and wind direction, air temperature at 2.5-m, longwave and short wave radiation are taken at the MetTower (down is negative). Fluxes are calculated using the observed surface pressure (at Florida one of the stations) rather than an assumed constant one. Wind direction is true and it accounts for the rotation of the tower during the year. Fluxes are also eliminated when the airflow was from the ship or through the tower. The data does include intercomparison calibrations done during the year and has been corrected based on the intercomparison and methods described in Persson et al. (2001).

The measurements of stress and sensible heat flux are the median values of the levels with "good" measurements. Eddy correlation measurements of the latent heat flux from the Ophir instruments are included, but are quite low with respect to bulk estimates so should be used with caution. The bulk estimates of stress, sensible and latent heat flux are calculated using a modified COARE flux algorithm that computes fluxes over the ocean or sea ice. For ice it uses Andreas 1987 for  $C_h$  and  $C_e$  it sets  $z_0=4.5e^{-4}$  m.

All values are averaged to daily means, and here we use mid-day (noon) time to choose positions. This approach allows a direct comparison to daily-averaged fields prescribed in the model. The atmospheric fields from ECMWF that we have used are:

- u/v winds at 10 meters (m/s) - used to derive air-ice stresses
- air temperature at 2 meters ( $T_{air}$ )
- incoming short wave ( $Q_{sw}$ ) and long wave ( $Q_{lw(down)}$ ) radiation fluxes
- moisture (dew point temperature) at 2 meters

In Figure 2 near-surface ECMWF air temperatures used to force the model are compared against SHEBA observations. The mean ECMWF air temperature at 2-m is close to those at 2.5-m from observations but they have significantly less short-term variability than data, especially during October - July period. In Figures 3 and

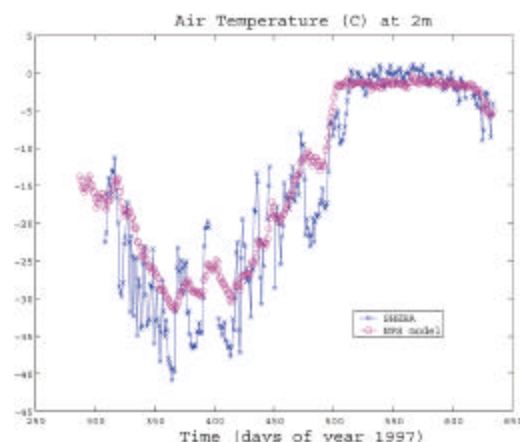


Figure 2. Air temperature along the SHEBA track from the NPS model (magenta) and from the observations (blue). The model air temperature is given at 2 m while the observations were made at 2.5 m.

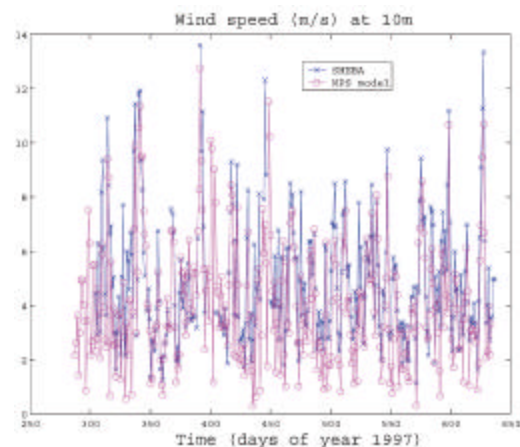


Figure 3. Wind speed at 10 m along the SHEBA track from the NPS model and from observations.

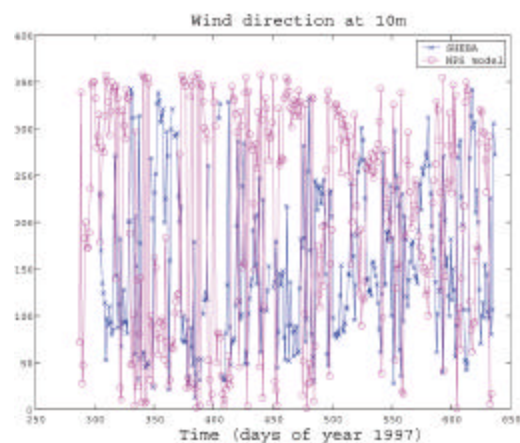


Figure 4. Wind direction at 10 m along the SHEBA track from the NPS model and from observations.

4 wind speed and direction are compared respectively. Wind speed is slightly underestimated in ECMWF and its variability is comparable with data. On the other hand, wind direction is quite different between the two sets. One of the reasons for this discrepancy might be associated with the fact that the model grid cell represents a 9 km x 9 km area and SHEBA data is measured at a point. In addition, ECMWF fields are interpolated to the 9-km model grid from a significantly lower resolution gridded output. This mismatch between the modeled and observed scales applies to all other parameters and at least in part contributes to model-data discrepancies.

Radiative fluxes (i.e. downward short and longwave radiation) are shown in Figures 5 and 6. Although the shortwave mean in the model is close to that from SHEBA data sets its variance is quite different, especially in summer. The longwave exhibits similar problems with the variance and in addition ECMWF values are usually smaller than those from SHEBA. As it was mentioned earlier, both spatial 'smoothing' and temporal averaging (to daily means) might be a part of the problem.

In Figure 7 we compare relative humidity. Since the model uses dewpoint temperature instead we computed an equivalent relative humidity based on  $T_{dew}$  and  $T_{air}$  from the NPS model:

$$RH = e/e_s * 100\%$$

$$e = e_o \exp[Lv/Rv (1/T_o - 1/T_d)]$$

$$e_s = e_o \exp[Lv/Rv (1/T_o - 1/T)]$$

where,

$e_o$  = reference saturation vapor pressure (=  $e_s$  at a certain temp = 6.11 hPa at usually 0°C)

$Lv$  = latent heat of vaporization of water ( $2.5 * 10^6$  Joules per kilogram)

$Rv$  = gas constant for water vapor (461.5 Joules / Kelvin / kilogram)

$T_o$  = reference temperature (273.15 Kelvin, Kelvin = °C + 273.15)

$T_d$  = dew point temperature (Kelvin)

$T$  = ambient air temperature (Kelvin)

This way calculated relative humidity is quite different (underestimated) compared to SHEBA data all year around with largest differences in winter. Temporal variability appears similar to data.

### 3.2 Sea Ice data

Next we compare NPS model derived ice fields with measurements from SHEBA. A 150-kHz narrow band RD Instruments Acoustic Doppler Current Profiler (ADCP) internally recorded 34,805 current ensembles in 362 days from an Ice-Ocean Environmental Buoy (IOEB) deployed during the SHEBA Experiment. The IOEB was initially deployed about 50 km from the main camp and drifted from 75.1°N, 141°W, to 80.6°N, 160°W, between October 1, 1997 and September 30, 1998. The ADCP was located at a depth of 14 m below the ice surface, and was configured to record data at 15 minute intervals from 40, 8m wide bins, extending downward 320 m below the instrument. The retrieved 24

Mbyte raw data are processed to remove noise, correct for platform drift and geomagnetic declination, remove

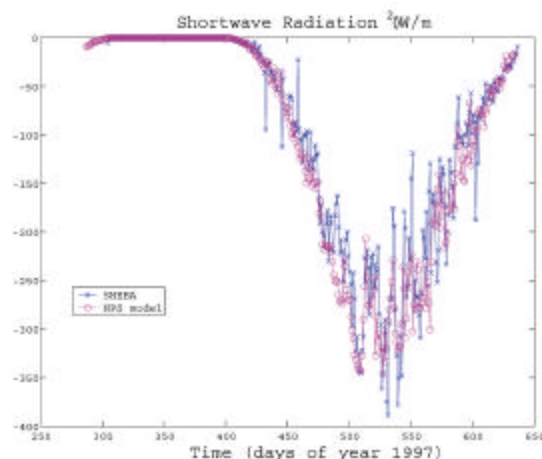


Figure 5. Incoming shortwave radiation along the SHEBA track and from the observations.

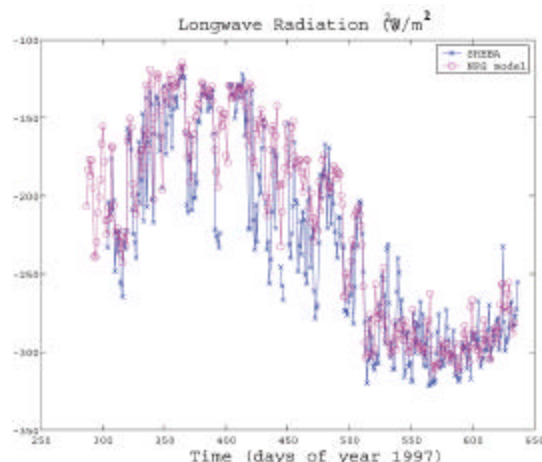


Figure 6. Incoming longwave radiation along the SHEBA track from the NPS model and from the observations.

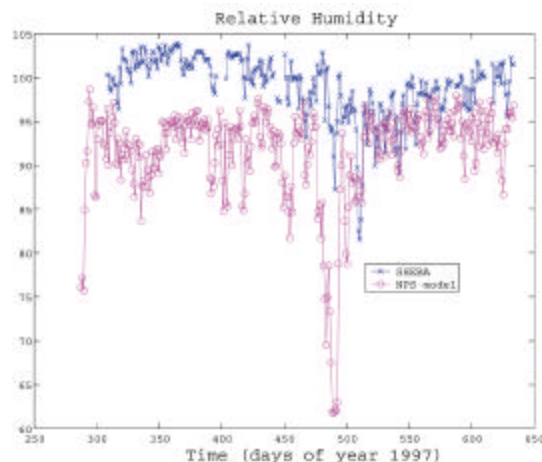


Figure 7. Dewpoint (moisture) temperature along the SHEBA track and from the observations.

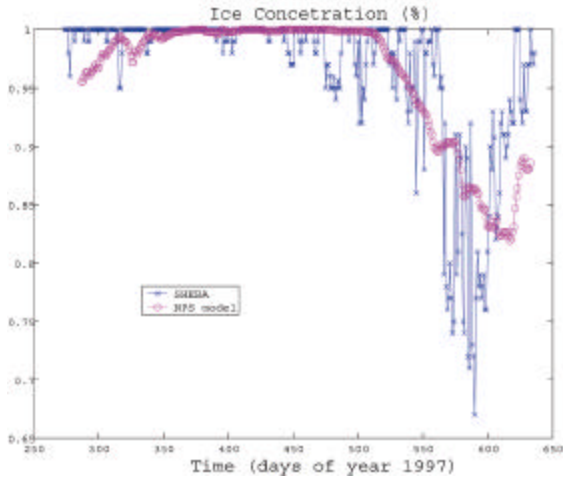


Figure 8. Ice concentration (%) along the SHEBA track from the NPS model and from the observations.

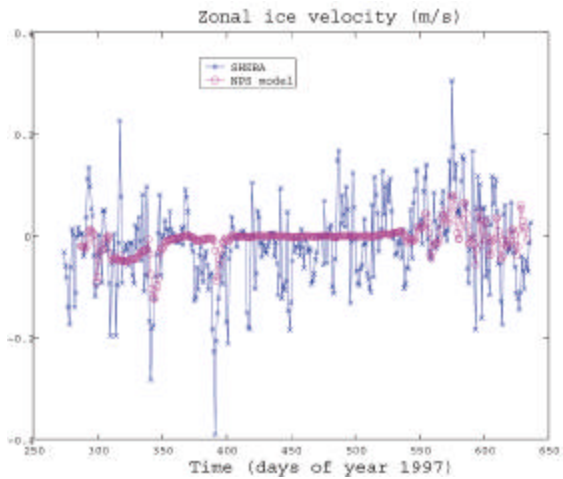


Figure 9. Zonal ice drift (m/s) along the SHEBA track from the NPS model and from the observations.

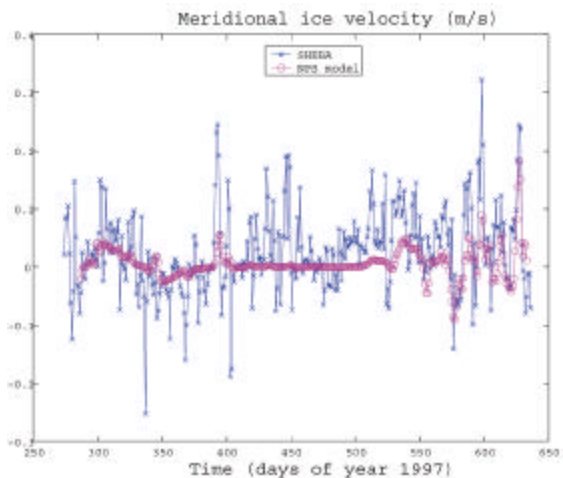


Figure 10. Meridional ice drift (m/s) along the SHEBA track from the NPS model and from the observations.

referenced current profiles along with ancillary data. Random errors in the 2 hr averaged ADCP measurements are estimated to be about 0.6 cm/s, while platform drift and Argos location uncertainty (~200 m) may introduces another 12 cm/s of error in the absolute currents.

The outgoing longwave and the turbulent heat fluxes are derived within the ice model by using the standard thermodynamic balance:

$$Q_o = Q_s + Q_l + \{Q_{lwdown} + Q_{lwup} + (1-a)(1-i_o)Q_{sw}\}$$

where,

$Q_s$  is the sensible heat flux,

$Q_l$  is the latent heat flux,

$Q_{lwdown}$  is the incoming longwave flux,

$Q_{lwup}$  is the outgoing longwave flux,

$Q_{sw}$  is the incoming shortwave flux,

$a$  is the shortwave radiation albedo,

and  $i_o$  is the fraction of absorbed shortwave flux that penetrates into the ice.

The outgoing longwave radiation flux is parameterized by the standard blackbody model

$$Q_{lwup} = \epsilon_s \sigma (T_{surface})^4$$

where,

$\epsilon_s$  is the emissivity of snow or ice (0.95),

$\sigma$  is the Stefan-Boltzmann constant,

and  $T_{surface}$  is the surface ice or snow temperature in degrees Kelvin.

The sensible heat is:

$$Q_s = C_s (\theta - T_{surface})$$

where,

$\theta$  is the air potential temperature and

$C_s$  is a nonlinear turbulent heat transfer coefficient.

The potential air temperature  $\theta$  is not provided as an ECMWF product, so the 2 meter air temperature can be substituted.

The latent heat flux is

$$Q_l = C_l (SPH - SPH_{surf})$$

where,

$SPH$  is the specific humidity provided by ECMWF,  $SPH_{surf} = 0.622$

$esat/p_o$  is the surface specific humidity

$p_o$  is a reference pressure and  $esat$  is a function of the surface temperature),

and  $C_l$  is the nonlinear turbulent latent heat transfer coefficient.

Putting it all together:

$$Q_o = C_s (T_{air} - T_{surf}) + C_l (SPH - SPH_{surf}) + \{Q_{lwdown} + \epsilon_s \sigma (T_{surface})^4 + (1-a)(1-i_o)Q_{sw}\}$$

where the fields  $Q_{wdown}$ ,  $Q_{sw}$ ,  $T_{air}$ , and humidity are provided by ECMWF.

\*The incoming shortwave radiation fluxes are available as products from ECMWF for the reanalysis period of 1979-1993, and after 1998. During the early reanalysis period only the net shortwave radiation flux was made available. The downward flux was originally backed out of the net flux by using the relation "albedo X net flux = downward flux". Using this relation produced a downward shortwave radiation flux with anomalous values inside of the Arctic basin. The magnitude of the downward shortwave radiation was typically half of its reanalysis values. It was eventually discovered that poor albedo estimates over the ice covered Arctic basin

were the cause of the bad downward flux values. Because there is extremely small variability year to year in the long wave and short wave radiation fluxes, multiple year averages were used to provide the downward values for 1994-1997.

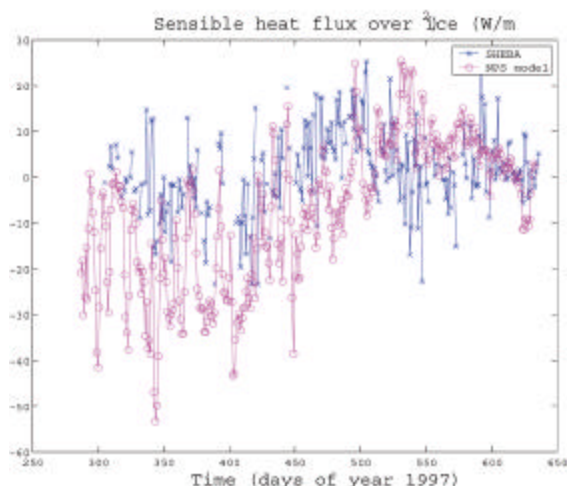


Figure 11. Sensible heat flux over ice ( $W/m^2$ ) along the SHEBA track from the NPS model and from observations.

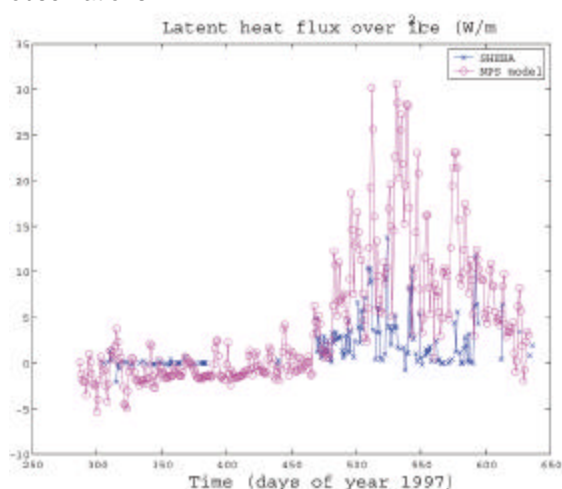


Figure 12. Latent heat flux over ice ( $W/m^2$ ) along the SHEBA track from the NPS model and from observations.

The rationale for calculating the sensible and latent heat fluxes within the model is to produce heat fluxes consistent with the ice conditions.

The model ice concentration throughout winter is 100% whereas SHEBA data show that there are frequent episodic reductions in the ice cover (Figure 8). Model results indicate that it takes overall a longer time to shift from winter to summer ice concentrations as compared to SHEBA data. Also the minimum ice concentrations occur later in the model than measured at the SHEBA station. Although the mean agrees with observations, the model does not reproduce the large concentration variability seen in observations.

Ice velocities (Figures 9 and 10) are significantly underestimated in the model. This is represented both

by almost no drift (ice appears to be locked in) in winter and as in the concentration field by much reduced variability compared to data. Recent comparison of a Hibler type sea ice model with a multi-category ice model (CICE) suggest that a part of the problem with too slow ice might be related to the ice strength parameterization tuned to a mean ice thickness in the former model (Maslowski and Lipscomb, 2003).

The model sensible heat flux (Figure 11) is significantly overestimated throughout the year, especially in winter when it is at least twice as large compared to data. In addition, its seasonal cycle appears to be about 1 month out of phase against the SHEBA measured cycle. The model latent heat flux (Figure 12) stays around  $0 W/m^2$  but it shows significantly overestimated variability in summer. These discrepancies will require detailed analyses of model forcing and thermodynamics parameters.

#### 4. SUMMARY

The SHEBA track is reproduced in great detail at the 9-km model horizontal resolution. Surface air temperatures are relatively well represented in the ECMWF data used to force the model, except they do not reproduce short term variability as shown in the observations. Wind speeds compare reasonably well against data but wind direction has significant discrepancies. We hypothesize that one of the reasons for that is that we compare a  $100 km^2$  averaged model grid cell information to a single point measurements. This argument applies to several other parameters used or calculated in the model. Both short and longwave downward radiative fluxes are quite realistic but again they are missing portions of higher frequency variability compared to data. Since the model uses dewpoint instead of relative humidity, differences between the model and observations might be related to the method of conversion of dewpoint to relative humidity as well as the skill of ECMWF operational products. Model predicted fields, including concentration and drift suggest that sea ice is much less energetic especially in winter. Other studies point to a need for an improved parameterization (tuning) of ice strength for a wide range of mean sea ice thicknesses. Discrepancies in model-data heat fluxes require further investigations.

#### REFERENCES

Bretherton, C.S., S.-R. de Roode, C. Jakob, E.L. Andreas, J. Intrieri, R.E. Moritz and P.Ola G. Persson, 2001: A comparison of the ECMWF forecast model with observations over the annual cycle at SHEBA, *J. Geophys. Res.* Submitted.

Beesley JA, Bretherton CS, Jakob C, Andreas EL, Intrieri JM, Uttal TA, 2000: A comparison of cloud and boundary layer variables in the ECMWF forecast model with observations at Surface Heat Budget of the Arctic Ocean (SHEBA) ice camp. *J. Geophys. Res. Atmos* 105 (D10): 12337-12349.

- Bitz, C. M., and W. H. Lipscomb, 1999: An energy conserving thermodynamic model of sea ice. *J. Geophys. Res.*, 104(C7), 15669-15677.
- Honjo, S., T. Takizawa, R. Krishfield, J. Kemp, and K. Hatakeyama, 1995, Drifting Buoys Make Discoveries About Interactive Processes in the Arctic Ocean, *EOS*, 76 (21) 209\& 215.
- Hunke, E.C., and J.K. Dukowicz, 1997: An elastic-viscous-plastic model for sea ice dynamics. *J. Phys. Oceanogr.*, 27:1849-1867.
- Krishfield, R., K. Doherty, and S. Honjo, Ice-Ocean Environmental Buoys (IOEB); Technology and Deployment in 1991 - 1992, WHOI Tech. Rep., WHOI-93-45, 1993.
- Krishfield, R., S. Honjo, T. Takizawa, and K. Hatakeyama, IOEB Archived Data Processing and Graphical Results from April 1992 through November 1998, WHOI Tech. Rep. WHOI-99-12, 1999.
- Lipscomb, W.H., 2001: Remapping the thickness distribution in sea ice models. *J. Geophys. Res.*, 106:13,989-14,000.
- Lipscomb, W.H., and E.C. Hunke, 2002: Modeling sea ice transport using incremental remapping. *Mon. Wea. Rev.*, submitted.
- Maslowski, W., W. Walczowski, 2002: On the circulation of the Baltic Sea and its connection to the Pan-Arctic region – a large scale and high-resolution modeling approach, *Boreal Environmental Research*, Vol.7, No.4, 319-326.
- Maslowski, W., and W.H. Lipscomb: High-resolution Simulations of Arctic Sea Ice During 1979-1993, *Polar Research*, accepted 2002.
- Maslowski, W., B. Newton, P. Schlosser, A. Semtner, and D. Martinson, 2000: Modeling recent climate variability in the Arctic Ocean. *Geophys. Res. Lett.*, 27(22), 3743-3746.
- Maslowski, W., D. C. Marble, W. Walczowski, and A. Semtner, 2001: On the large scale shifts in Arctic Ocean and sea-ice conditions during 1979-98. *Annals of Glaciology*, 33, 545-550.
- Persson POG, Fairall CW, Andreas EL, Guest PS, Perovich DK, 2002: Measurements near the Atmospheric Surface Flux Group tower at SHEBA: Near-surface conditions and surface energy budget, *J. Geoph. Res.-Oceans*, 107 (C10): art. no. 8045 SEP-OCT 2002
- Takizawa, T., K. Hatakeyama, T. Nakamura, S. Honjo, R. Krishfield, and N. Koyama, Report of Arctic Observational Data by Ice-Ocean Environmental Buoys (IOEB) 1 and 2 (April 1992 to July 1995), JAMSTEC Technical Report, August 1995 (in Japanese).
- Uttal, T., J.A. Curry, M.G. McPhee, D.K. Perovich, R.E. Moritz, J.A. Maslanik, P.S. Guest, H.L. Stern, J.A. Moore, R. Turenne, A. Heiberg, M.C. Serreze, D.P. Wylie, O.G. Persson, C.A. Paulson, C. Halle, J.H. Morison, P.A. Wheeler, A. Makshtas, H. Welch, M.D. Shupe, J.M. Intrieri, K. Stamnes, R.W. Lindsey, R. Pinkel, W.S. Pegau, T.P. Stanton, T.C. Grenfeld, 2002: Surface heat budget of the Arctic Ocean, *Bulletin of the American Meteorological Society* 83 (2), 255-275.